# High-density horizontally aligned growth of carbon nanotubes with Co nanoparticles deposited by arc-discharge plasma method

D. Phokharatkul,[1] Y. Ohno,[1,a)] H. Nakano,[2] S. Kishimoto,[1] and T. Mizutani[1]
[1]*Department of Quantum Engineering, Nagoya University, Furo-cho, Chikusa-ku, Nagoya 464-8603, Japan*
[2]*Tsukuba Institute for Super Materials, ULVAC, Inc., 5-9-6 Tohkohdai, Tsukuba 300-2635, Japan*

(Received 21 April 2008; accepted 18 July 2008; published online 7 August 2008)

High-density horizontally aligned single-walled carbon nanotubes are grown on a quartz substrate using Co nanoparticles deposited by arc-discharge plasma method. The Co nanoparticles with a density as high as $6.0\times10^{10}$ cm$^{-2}$ are formed by a single pulse of arc discharge at room temperature. The density of the aligned nanotubes is $\sim$8 $\mu$m$^{-1}$ in average. Multichannel nanotube field-effect transistors with a high-*k* top-gate structure are fabricated with aligned nanotubes. The devices show high-performance, normally on, and *n*-type conduction property without any doping process. A high on current of 1.3 mA and a large transconductance of 0.23 mS for a channel width of 100 $\mu$m are obtained. The normally on and *n*-type property is attributed to fixed positive charges in the $HfO_2$ gate insulator and at the interfaces. © *2008 American Institute of Physics*.
[DOI: 10.1063/1.2969290]

Semiconducting single-walled carbon nanotubes (SWNTs) have attracted much attention because of their potentials for nanotransistor applications with advantages such as high speed operation and high current density. Recently, high-frequency operation with a cutoff frequency of 30 GHz has been demonstrated in carbon nanotube field-effect transistors (CNFETs).[1] However, the demonstrated operating frequency is still much lower than the terahertz-range expected from the intrinsic carrier velocity of SWNTs.[2,3] This is mostly because of the small current driving capability of CNFETs against the parasitic capacitances attributed to the electrodes and the wirings.

The high-density alignment of SWNT channels is the most efficient approach to increase current driving capability of CNFETs. So far, horizontally aligned SWNTs can be grown by fast heating,[4] electric-field assisted growth,[5] and growth on crystalline oxide substrates.[6–9] Among these, the alignment technique with crystalline oxide substrates such as sapphire and quartz has advantages for high-density packing of SWNTs without bundling and for large-scale production. Ismach *et al.*[6] and Han *et al.*[7] independently reported the aligned growth of SWNTs guided by atomic steps of sapphire substrate. Almost at the same time, Ago *et al.* also reported aligned growth of SWNTs along atomic arrays of Al on *A*-plane and *R*-plane sapphire substrates.[8] The denser aligned SWNTs with better degree of alignment were grown on ST-cut quartz substrate with ferritine as the catalyst by Kocabas *et al.*[9] Although the aligned-growth techniques have been advancing, the density is still not enough for the high-speed device applications.

The preparation of high-density and nanosized catalyst particles is one of the key points for high-density growth of SWNTs. For device application, solution techniques such as dip coating[10] are not suitable at the points of controllability and uniformity. The electron-beam (EB) evaporation and subsequent segregation in high temperature are often used for the preparation of catalysts pattern on a substrate. The controllability of the density and size of the produced particles is poor because of the large migration rate of the metal on the surface of oxide substrates.

In this study, we introduce arc-discharge plasma (ADP) for the high-density deposition of catalytic nanoparticle. We grow horizontally aligned SWNTs on ST-cut quartz substrate by alcohol catalytic chemical vapor deposition (ACCVD).[11] We also fabricate high-performance *n*-type multichannel CNFETs with a high-*k* top-gate structure. The origin of *n*-type conduction property is discussed.

ST-cut quartz substrate was used to grow horizontally aligned SWNTs. The substrate was annealed at 900 °C for 8 h in air.[9] After the photoresist patterning of catalysts on the substrate, Co nanoparticles were deposited by ADP, which is a kind of vacuum evaporation technique that evaporates the cathode material by arc discharge in vacuum.[12] As shown in Fig. 1, the ADP gun consists of a cathode rod made of the evaporating material and an anode electrode in a coaxial arrangement. Triggered-pulse ADP was used in this study. The film thickness can be controlled by a number of pulse discharges. The controllability and reproducibility of the thickness of very thin film are superior to the EB evaporation method. By a single pulse discharge, high-density Co particles were obtained at room temperature, as shown in Fig. 2(a). The mean thickness of Co film deposited for a single pulse discharge was 0.2 nm, which was estimated from the thickness of a thick film deposited for discharges of 50 pulses. The density of the nanoparticles is $6.0\times10^{10}$ cm$^{-2}$. The height distribution is shown in Fig. 2(b). The average and standard deviation are 1.06 and 0.41 nm, respectively. The density of the Co nanoparticles was much higher than

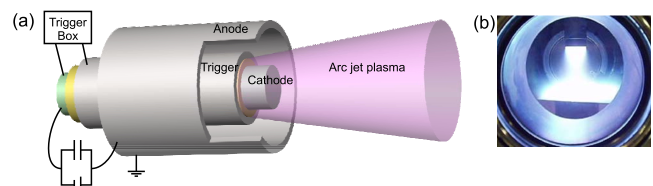


FIG. 1. (Color online) (a) Schematic and (b) photograph of ADP gun used for deposition of Co nanoparticles.

a)Electronic mail: yohno@nuee.nagoya-u.ac.jp.

 © 2008 American Institute of Physics

Downloaded 28 Jul 2009 to 133.6.32.19. Redistribution subject to AIP license or copyright; see http://apl.aip.org/apl/copyright.jsp

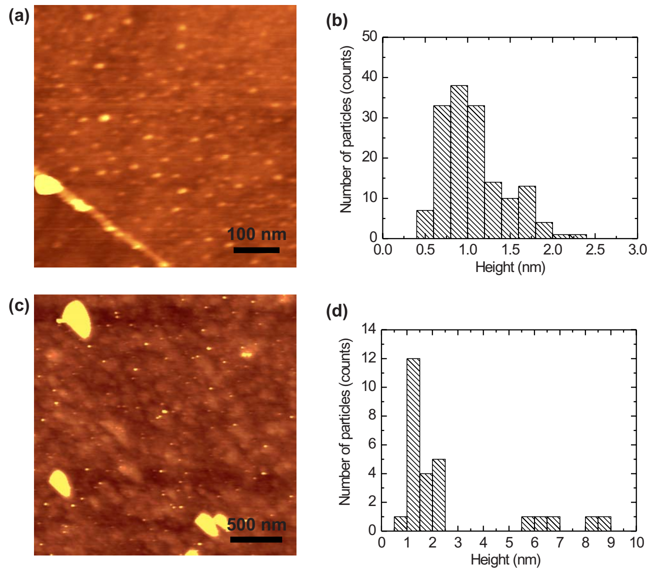


FIG. 2. (Color online) (a) AFM image and (b) height distribution of Co particles deposited by ADP. The line crossing on the lower left in (a) is the residual photoresist at the edge of photolithographic pattern. (c) and (d) are those of Co particles deposited by EB evaporation after annealed at 800 °C.

that obtained by the EB evaporation and subsequent segregation at high temperature. As shown in Figs. 2(c) and 2(d), although Co particles with a height of 1–2 nm were produced from 0.5-nm-thick Co film deposited by EB evaporation method by annealing at 800 °C, the density of Co particles was suppressed in the order of $2\times10^9$ cm$^{-2}$. This is because most of Co metal migrates with high migration rate on the quartz surface and forms large particles with a height more than 5 nm, as shown in Fig. 2(d). In the case of the ADP, the incident metal atoms with relatively high energy of a few tens of eV have strong adhesion to the substrate and form high-density nuclei, and then the nanoparticles are produced on the substrate.

SWNTs were grown by ACCVD with ethanol of 150 SCCM (SCCM denotes standard cubic centimeter per minute at STP) at 5 Torr and 800 °C for 60 min. To suppress cohesion of Co nanoparticles at the high temperature, the temperature of the furnace was raised in oxidization atmosphere by feeding ambient air. As shown in Fig. 3, high-density and horizontally aligned SWNTs were obtained. The density is ~8 $\mu$m$^{-1}$ in average and partially more than 10 $\mu$m$^{-1}$. Even though we did not employ any reduction processes before feeding ethanol gas, such high-density SWNTs were grown from the Co particles. The Co particles seem to be reduced by the ethanol or the decomposed species such as hydrogen and $C_2H_2$.[13] We examined the intentional reduction of the oxidized Co with hydrogen to activate the catalysts more efficiently. However, the density of aligned SWNTs was decreased, and the degree of alignment became worse with reduction time, even in short time of ~5 s. This is probably due to the cohesion of Co nanoparticles. Because of such uncontrollability originating from high migration rate of the reduced metal Co on a quartz substrate, the present procedure to deposit nanoparticles at room temperature using ADP and to raise temperature in oxidizing atmosphere is effective to prepare catalysts suitable for the growth of high-density aligned SWNTs. As shown in Fig. 3(b), the degree of the alignment is relatively low as compared to previous report.[9] We speculate that this is due to the surface roughness of the quartz substrate used in this study.

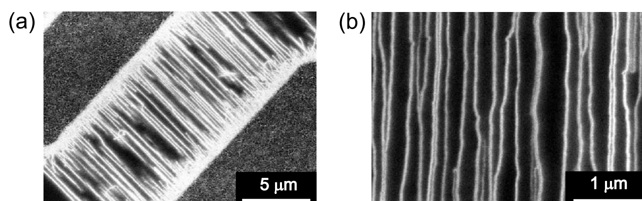


FIG. 3. SEM images of SWNTs grown on quartz substrate.

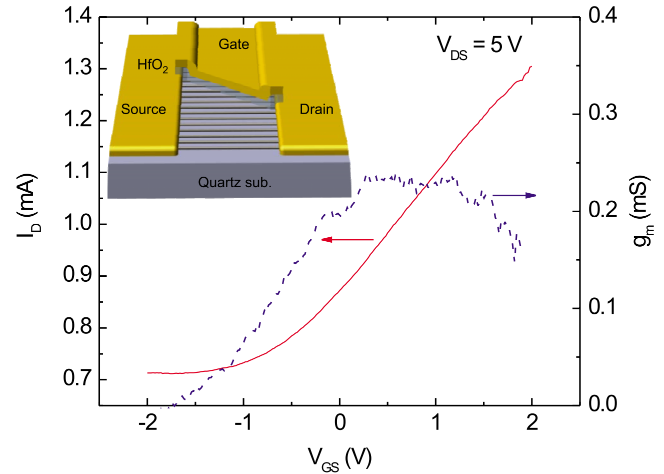


FIG. 4. (Color online) $I_D$ and $g_m$ as a function of $V_{GS}$ at $V_{DS}$=5 V. The inset shows a schematic of fabricated multichannel CNFET with high-$k$ top-gate structure.

Multichannel CNFETs with high-$k$ top-gate structure were fabricated using the aligned SWNTs. The schematic device structure is shown in the inset of Fig. 4. After the growth of SWNTs, the source and drain electrodes of Au (100 nm) were formed. The 30-nm-thick $HfO_2$ gate insulator was deposited by atomic-layer deposition (ALD) at 250 °C. Finally, the top-gate electrode of Au/Ti (250/50 nm) was formed. The channel length ($L_{ch}$) and width ($W_{ch}$) were 2 and 100 $\mu$m, respectively. In the present devices, the average density of SWNTs was relatively low as ~3 $\mu$m$^{-1}$.[14]

The drain current ($I_D$) and transconductance ($g_m$) are shown in Fig. 4 as a function of gate-source voltage ($V_{GS}$) at the drain-source voltage ($V_{DS}$) of 5 V. The transfer characteristics show normally on and $n$-type conduction with a threshold voltage ($V_{th}$) of −1.6 V. The maximum $I_D$ and $g_m$ are 1.3 mA and 0.23 mS, respectively. The $I_D$ and $g_m$ normalized by $W_{ch}$ are 13 mA/mm and 2.3 mS/mm, respectively, which are the highest values for $n$-type multichannel CNFETs to our knowledge. Much higher values can be obtained for single-channel $n$-type devices if they are normalized by the diameter of SWNT.[15] Even though such $g_m$ normalized by the diameter of SWNT implies the intrinsic potential of CNFETs, the $g_m$ per unit $W_{ch}$ should be considered as a figure of merit from a viewpoint of high-speed operation of FETs, since the operation speed of the device is generally limited by parasitic capacitances of electrodes and wirings. In the present devices, there is still room to improve device performance by increasing the density of SWNTs and reducing the $L_{ch}$. The on/off ratio is 1.8. The off current is due to metallic SWNTs.

Downloaded 28 Jul 2009 to 133.6.32.19. Redistribution subject to AIP license or copyright; see http://apl.aip.org/apl/copyright.jsp

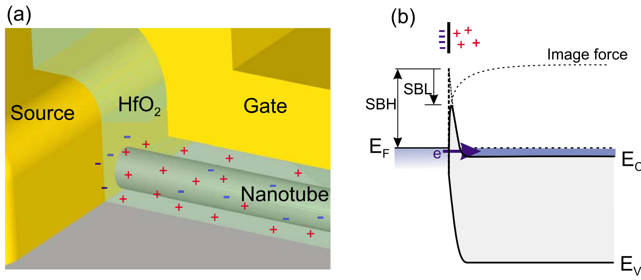


FIG. 5. (Color online) (a) Bird's eye-view illustration and energy-band diagram at source contact.

From the *n*-type and normally on conduction property, we can speculate that the Schottky barrier formed at the interface between the SWNT and source contact is small for electrons and that electrons are doped in the SWNT even though any doping processes is not introduced in the present device fabrication. The carrier type of the device changed from *p*-type to *n*-type during the deposition of the gate insulator by ALD. This cannot be explained by desorption of oxygen adsorbed in the vicinity of the contact interface[16] alone, since the work function of the contact metal ($\phi_{Au}$ =5.2 eV) is larger than that of SWNTs ($\phi_{NT}$=4.8 eV). The energy band alignment at the contact interface can be modified by the dipole which is formed by molecules adsorbed in the vicinity of the metal/SWNT interface.[16–18] For instance, in CNFETs, oxygen molecules would induce the dipole layer so as to induce an abrupt band bending at the interface, leading to an increase in the effective work function of metal. This results in a reduction of the Schottky barrier height and the contact resistance for *p*-type conduction. Such abrupt band bending can also be introduced by fixed charges around the interface, which changes the Schottky barrier thickness similar to the depletion layer of doped semiconductors. To decrease Schottky barrier thickness for electrons, positive fixed charges should be introduced to overcome the difference of bear work functions of Au and SWNT in the present device.

Such positive fixed charges can be introduced by the $HfO_2$ deposited by ALD as previous experimental observations.[19,20] As illustrated in Fig. 5(a), the electric force lines diverging from the positive charges near the contact electrodes are terminated at the source contact, forming high field in the Schottky barrier. This results in an abrupt band bending in the Schottky barrier and a reduction of the Schottky barrier thickness for electrons, as shown in Fig. 5(b). In the case of such thin Schottky barrier, the Schottky barrier lowering due to image force effect becomes significant, enhancing electron tunneling probability. The normally on characteristics are one of the evidences of the existence of the positive fixed charges around the SWNT channel. The positive fixed charges act as a kind of electron dopant via Coulomb force (electrostatic doping), and the Fermi energy ($E_F$) of SWNT channel rise up into the conduction band at zero $V_{GS}$. Electrostatic doping may also be caused by the work function difference between the SWNT and gate electrode ($\phi_{Ti}$=4.3 eV). However, the small difference in the work functions cannot be a dominant factor in such deep negative $V_{th}$ as −1.6 V.

So far, chemical doping with K,[21] annealing in vacuum,[22] contact with small work function metal such as Ca (Ref. 17) and Sc (Ref. 23) have been suggested for the realization of *n*-type CNFETs, but these devices are unstable in air or affected by environmental condition. In the case of the present device, on the other hand, the conduction property is quite stable because the gate insulator acts as a passivation film, and also the top gate metal screens the electric field attributed to environmental molecules such as water.

In summary, it has been shown that the ADP was useful to deposit high-density Co nanoparticles for the catalysts in the growth of SWNTs. By suppressing the migration of the nanoparticles during raising temperature in air, high-density aligned SWNTs were grown by alcohol catalytic CVD. The fabricated multichannel CNFETs with high-*k* top-gate structure showed normally on and *n*-type transfer characteristics with a high on current of 13 mA/mm and $g_m$ of 2.3 mS/mm. The normally on and *n*-type characteristics were attributed to the positive fixed charges in the $HfO_2$ film and/or at the interfaces.

This work is partially supported by SCOPE of MIC, Grant-in-Aid for Scientific Research on Priority Area of MEXT, and Innovation Research Project on Nanoelectronics Materials and Structures of METI.

[1] A. L. Louarn, F. Kapche, J.-M. Bethoux, H. Happy, G. Dambrine, V. Derycke, P. Chenevier, N. Izard, M. F. Goffman, and J.-P. Bourgoin, Appl. Phys. Lett. **90**, 233108 (2007).
[2] P. J. Burke, Solid-State Electron. **48**, 1981 (2004).
[3] S. Hasan, S. Salahuddin, M. Vaydyanathan, and M. A. Alam, IEEE Trans. Nanotechnol. **5**, 14 (2006).
[4] S. Huang, X. Cai, and J. Liu, J. Am. Chem. Soc. **125**, 5636 (2003).
[5] Y. Zhang, A. Chang, J. Cao, Q. Wang, W. Kim, Y. Li, N. Morris, E. Yenilmez, J. Kong, and H. Dai, Appl. Phys. Lett. **79**, 3155 (2001).
[6] A. Ismach, L. Segev, E. Wachtel, and E. Joselevich, Angew. Chem. **116**, 6266 (2004).
[7] S. Han, X. Liu, and C. Zhou, J. Am. Chem. Soc. **127**, 5294 (2005).
[8] H. Ago, K. Nakamura, K. Ikeda, N. Uehara, N. Ishigami, and M. Tsuji, Chem. Phys. Lett. **408**, 433 (2005).
[9] C. Kocabas, S. H. Hur, A. Gaur, M. A. Meitl, M. Shim, and J. A. Rogers, Biophys. J. **1**, 1110 (2005).
[10] Y. Murakami, Y. Miyauchi, S. Chiashi, and S. Maruyama, Chem. Phys. Lett. **377**, 49 (2003).
[11] S. Maruyama, R. Kojima, Y. Miyauchi, S. Chiashi, and M. Kohno, Chem. Phys. Lett. **360**, 229 (2002).
[12] Y. Agawa, K. Yamaguchi, Y. Hara, S. Amano, T. Horiuchi, and G. Shen, ULVAC Tech. J. **57E**, 1 (2003).
[13] J. Park, R. S. Zhu, and M. C. Lin, J. Chem. Phys. **117**, 3224 (2002).
[14] This is a technical problem attributing to the photomask used in this study, where the pattern of catalysts was placed only on the one side of the contact electrodes.
[15] A. Javey, R. Tu, D. B. Farmer, J. Guo, R. G. Gordon, and H. Dai, Nano Lett. **5**, 345 (2005).
[16] S. Heinze, J. Tersoff, R. Martel, V. Derycke, J. Appenzeller, and P. Avouris, Phys. Rev. Lett. **89**, 106801 (2002).
[17] Y. Nosho, Y. Ohno, S. Kishimoto, and T. Mizutani, Appl. Phys. Lett. **86**, 073105 (2005).
[18] Y. Nosho, Y. Ohno, S. Kishimoto, and T. Mizutani, Nanotechnology **18**, 415202 (2007).
[19] R. S. Johnson, G. Lucovski, and I. Baumvol, J. Vac. Sci. Technol. A **19**, 1353 (2001).
[20] D.-G. Park, H.-J. Cho, K.-Y. Lim, C. Lim, I.-S. Yeo, J.-S. Roh, and J. W. Park, J. Appl. Phys. **89**, 6275 (2001).
[21] M. Bockrath, J. Hone, A. Zettl, P. L. McEuen, A. G. Rinzler, and R. E. Smalley, Phys. Rev. B **61**, R10606 (2000).
[22] V. Derycke, R. Martel, J. Appenzeller, and Ph. Avouris, Nano Lett. **1**, 453 (2001).
[23] Z. Zhang, X. Liang, S. Wang, K. Yao, Y. Hu, Y. Zhu, Q. Chen, W. Zhou, Y. Li, Y. Yao, J. Zhang, and L.-M. Peng, Nano Lett. **7**, 3603 (2007).

**Downloaded 28 Jul 2009 to 133.6.32.19. Redistribution subject to AIP license or copyright; see http://apl.aip.org/apl/copyright.jsp**